



1 Estimating Satellite and Receiver Differential Code Bias Using Relative GPS Network

2 Alaa A. Elghazouly¹, Mohamed I. Doma¹, Ahmed A. Sedeek²

3 1. Faculty of Engineering, Menoufia University, Egypt.
 4 2. EL Behira Higher Institute of Engineering and Technology, El Behira, Egypt.

5 Abstract

6 Precise Total Electron Content (TEC) are required to produce accurate spatial and temporal resolution of Global Ionosphere
 7 Maps (GIMs). Receivers and Satellites Differential Code Biases (DCBs) are one of the main error sources in estimating precise
 8 TEC from Global Positioning Systems (GPS) data. Recently, researchers are interested in developing models and algorithms
 9 to compute DCBs of receivers and satellites close to those computed from the Ionosphere Associated Analysis Centers
 10 (IAAC). Here we introduce a MATLAB code called Multi Station DCB Estimation (MSDCBE) to calculate satellites and
 11 receivers DCBs from GPS data. MSDCBE based on spherical harmonic function and geometry free combination of GPS
 12 carrier phase and pseudo-range code observations and weighted least square were applied to solve observation equations, to
 13 improve estimation of DCBs values. There are many factors affecting estimated value of DCBs. The first one is the
 14 observations weighting function which depending on the satellite elevation angle. The second factor concerned with estimating
 15 DCBs using single GPS Station Precise Point Positioning (PPP) or using GPS network. The third factor is the number of GPS
 16 receivers in the network. Results from MSDCBE were evaluated and compared with data from IAAC and other codes like
 17 M_DCB and ZDDCBE. The results of weighted (MSDCBE) least square shows an improvement for estimated DCBs, where
 18 mean differences from CODE less than 0.746 ns. DCBs estimated from GPS network shows a good agreement with IAAC
 19 than DCBs estimated from PPP where the mean differences are less than 0.1477 ns and 1.1866 ns, respectively. The mean
 20 differences of computed DCBs improved by increasing number of GPS stations in the network.

21 **Keywords:** DCBs, Multi station, elevation angle, number of stations.

22 1. Introduction

23 TEC is an important parameter in the study of ionospheric dynamics, structures, and variabilities. The dispersive nature of the
 24 ionosphere at UHF frequencies allows for the calculation of TEC using GPS dual-frequency radio transmissions. The global
 25 availability of GPS has made it a valuable tool in regional and global TEC estimation. Unfortunately, GPS-derived TEC
 26 measurements are adversely affected by an inherent interfrequency bias within the receiver and satellite hardware, typically
 27 referred to as the DCBs. Careful estimation of the DCBs is required to obtain accurate TEC, which is used in several
 28 applications, such as in several ionospheric prediction models, and in the correction of GPS positioning measurements
 29 (McCaffrey et al., 2017). A number of methods have been proposed for the estimation of GPS receiver DCBs, each with
 30 varying requirements and limitations including: making assumptions about the ionospheric structure; the use of internal
 31 calibration; or the use of a reference instrument or model. Estimating DCBs for receivers and satellites from GPS observations
 32 depending on two approaches, the relative and absolute methods. The relative method utilizes a GPS network, while the
 33 absolute method determines DCBs from a single station (Sedeek et al., 2017). **In the current study** we applied relative method
 34 to calculate DCBs of satellites and GPS receivers.

35 There has also been growing interest in measuring the accuracy of these methods, and how different factors, e.g. ionospheric
 36 activity, plays a role in these methods (McCaffrey et al., 2017). Nowadays, accurate DCBs of satellites and IGS stations can
 37 be obtained from IAAC like CODE (University of Bern, Switzerland), European Space Agency (ESA, Germany), Jet
 38 Propulsion Laboratory (JPL, USA), and UPC (Technical University of Catalonia, Spain). However, the availability of IAAC
 39 BCB values but it is only available for IGS stations only. Furthermore, some of IGS ground receiver DCB estimates are not
 40 available from all analysis centers. Also, some regions don't have any IGS ground stations like our country Egypt, which mean
 41 the TEC values over them would be interpolated from nearest calculated values. As TEC values depended on DCB values it
 42 is required a mathematical model to calculate DCBs from GPS data.

43
 44 In this study we introduce a mathematical model estimating satellites & receiver DCBs for A GPS network based on Spherical
 45 Harmonic function (SHF) written under MATLAB environment, the developed mathematical model uses geometry free
 46 combination of pseudo-range observables (P-code). Weighted Least Square was used to consider variation of satellites
 47 elevation angle. The code was evaluated and compared with other researchers' codes in section "Results and analysis". In the
 48 "Conclusion" section we summarize the overall paper results.

49 2. GPS Observation Model

50 For a GPS satellite, the pseudorange and carrier phase observations between a receiver and a satellite can be expressed as (Jin
 51 et al., 2008; Leandro, 2009; Leick et al., 2015; Zhang et al., 2018):

$$52 P_{r,j}^s(i) = \rho_r^s(i) + c(dt_r - dt^s) + T_r^s + I_{r,j,p}^s + DCB_r^p - DCB_s^p + M_j + E_j \quad (1)$$

$$53 \Phi_{r,j}^s(i) = \rho_r^s(i) + c(dt_r - dt^s) + T_r^s - I_{r,j,\phi}^s + \lambda_j N_j + pb_{r,j} - pb_{s,j} + DCB_r^\phi - DCB_s^\phi + m_j + e_j \quad (2)$$



54	With r, s, j and i the receiver, satellite, frequency and epoch indices, and where:
55	$P_{r,j}^s(i)$ Pseudo-range measurements, in meter,
56	$\Phi_{r,j}^s(i)$ carrier-phase measurements, in meter,
57	$\rho_r^s(i)$ the geometric distance between satellite and receiver antennas, in meters,
58	c the speed of light, in meters per second,
59	dt_r and dt^s receiver and satellite clock errors, respectively, in seconds,
60	T_r^s the neutral troposphere delay, in meters,
61	$I_{r,j,p}^s$ and $I_{r,j,\phi}^s$ the ionosphere delay of pseudo range and carrier phase observations, in meters,
62	N_j carrier-phase integer ambiguities, in cycles,
63	λ_j carrier-phase wave length, in meters,
64	DCB_r^p and DCB_s^p receiver and satellite pseudo-range hardware delays, respectively in metric units,
65	DCB_r^ϕ and DCB_s^ϕ receiver and satellite carrier-phase hardware delays, respectively, in metric units,
66	M_j Pseudo-range multipath on, in meters,
67	E_j Other un-modeled errors of pseudo-range measurements, in meters,
68	pbr,i and pbs,i receiver and satellite carrier-phase initial phase bias, respectively, in metric units,
69	m_j carrier-phase multipath, in meters and
70	e_j Other un-modeled errors of carrier-phase measurements, in meters.

71 Here, we consider a measurement scenario that one GPS receiver tracks dual frequency code and phase data from a total of m
 72 satellites over t epochs, thereby implying $r = 1, s = 1, \dots, m, j = 1, 2$ and $i = 1, \dots, t$.

73 Firstly, the code read the Rinex files and extract the pseudo range and carrier phase observations which are the range distances
 74 between the receivers and satellites measured using L_1 and L_2 frequencies. The “geometry-free” linear combination of GPS
 75 observations is used to derive the observable. The geometric range, clock-offsets and tropospheric delay are frequency
 76 independent and can be eliminated using this combination. The “geometry-free” linear combinations for pseudo range and
 77 carrier phase observations are given as (Al-Fanek 2013):

$$78 P_4 = P_{r,1}^s(i) - P_{r,2}^s(i) = I_{r,1,p}^s - I_{r,2,p}^s + DCB_r^p + DCB_s^p + E_{12} \quad (3)$$

$$79 \Phi_4 = \Phi_{r,1}^s(i) - \Phi_{r,2}^s(i) = I_{r,2,\phi}^s - I_{r,1,\phi}^s + \lambda_1 N_1 - \lambda_2 N_2 + DCB_r^\phi + DCB_s^\phi + e_{12} \quad (4)$$

80 $E_{12} = \sqrt{(E_1)^2 + (E_2)^2}$ is the combination of multipath and measurement noise on $P_{r,1}^s(i)$ and $P_{r,2}^s(i)$ (m) and

81 $e_{12} = \sqrt{(e_1)^2 + (e_2)^2}$ is the combination of multipath and measurement noise on $\Phi_{r,1}^s(i)$ and $\Phi_{r,2}^s(i)$ (m).

82 To reduce the multipath and noise level in the pseudo range observables, the carrier phase measurements are used to compute
 83 a more precise relative smoothed range. Although the carrier-phase observables are more precise than the code derived, they
 84 are ambiguous due to the presence of integer phase ambiguities in the carrier phase measurements. To take advantage of the
 85 low-noise carrier phase derived and unambiguous nature of the carrier phase, both measurements are combined to collect the
 86 best of both observations.

87 Smoothed $P_{4,sm}$ observations can be expressed as follows (Jin et al. 2012):

$$88 P_{4,sm} = \omega_t P_4(t) + (1 - \omega_t) P_{4,prd}(t) \quad (t > 1) \quad (5)$$

89 where t stands for the epoch number, ω_t is the weight factor related with epoch t , and

$$90 P_{4,prd}(t) = P_{4,sm}(t-1) + [L_4(t) - L_4(t-1)] \quad (t > 1) \quad (6)$$

91 when t is equal to 1, which means the first epoch of one observation arc, $P_{4,sm}$ is equal to P_4 .

93 3. Spherical Harmonic Model

94 To determine the receiver DCB, there are two different methods. The first one is to calibrate the receiver device and obtain the
 95 DCB directly. This method calculates the DCB of the receiver device ignoring that from the antenna cabling used during
 96 observation (Hansen, 2002). The second method calculates the receiver DCB as a part of GPS signal time delay which is
 97 independent on type of antenna. MSDCBE code works as the second methods (figure 1).

98 The ionosphere delay can be expressed as follows (Abid et al. 2016):

$$99 d_{ion} = \frac{40.3}{f^2} STEC \quad (7)$$

100 Where f stands for the frequency of the carrier and STEC is the total electron content along the path of the signal. The
 101 observation equation can be formed by Substituting (9) into (7), and replacing P_4 by

102 smoothed $P_{4,sm}$, we get (Abid et al. 2016):

$$103 P_{4,sm} = 40.3 \left(\frac{1}{f_1^2} - \frac{1}{f_2^2} \right) STEC + c * DCB_r + c * DCB_s \quad (8)$$

104 Where: c is the speed of light and DCB_r and DCB_s are differential code bias for receiver and satellites in seconds.

105 STEC can be translated into vertical total electron content (VTEC) using the modified single-layer model (MSLM) (Haines
 106 1985, Jin et al. 2012):



107 $VTEC = MF(z)STEC$ (9)

108 $MF = \cos\left(\arcsin\left(\frac{R}{R+H}\sin(\alpha z)\right)\right)$ (10)

109 Where:

110 MF is the mapping function,

111 z is the satellite elevation angle,

112 R is the radius of the Earth=6371 km and

113 H is the attitude of the ionosphere thin shell (assumed as used by CODE=506.7 km), $\alpha=0.9782$.

114 To estimate the satellite and receiver HDs, the current study applies a model based on spherical harmonic function to calculate
 115 them using zero-difference observations. The used model is expressed as follows (Schaer 1999, Li et al. 2015):

116 $VTEC(\beta, s) = \sum_{n=0}^N \sum_{m=0}^n P_n^m(\sin(\beta))(A_n^m \cos(m\lambda) + B_n^m \sin(m\lambda))$ (11)

117 Where:

118 β is the geocentric latitude of IPPs (Ionosphere Peirce Point),

119 s is the solar fixed longitude of IPPs,

120 N is the degree of the spherical function,

121 M is the order of spherical harmonic function,

122 P_{nm} is regularization Legendre series and

123 A_{nm} and B_{nm} are the estimated spherical harmonics coefficients.

124 By substituting eq (11) and eq (13) into eq (10) we get:

125
$$\sum_{n=0}^N \sum_{m=0}^n P_n^m(\sin(\beta))(A_n^m \cos(m\lambda) + B_n^m \sin(m\lambda))$$

 126
$$= \cos\left(\arcsin\left(\frac{R}{R+H}\sin(\alpha z)\right)\right) \left[-\frac{f_1^2 f_2^2}{40.3(f_1^2 - f_2^2)}(P_{4,sm} - c * DCB_r - c * DCB_s)\right]$$
 (12)

127 Only one GPS station has 20,000 observations per a day. When applying equation (12) using stations observation data, there
 128 are number of equations much more than the number of unknown coefficients. These coefficients were determined using
 129 weighted least square method. general form of weighted least square function can be expressed as (Ghilani and Wolf, 2012):

130 $X = (A^T P A)^{-1} A^T P L$ (13)

131 Where:

132 X is the unknown parameters vector namely, A_n^m, B_n^m, DCB_r and DCB_s ,

133 A is the coefficient (design) matrix (coefficients of A_n^m, B_n^m, DCB_r and DCB_s),

134 L is the observation vector (values of $P_{4,sm}$) and

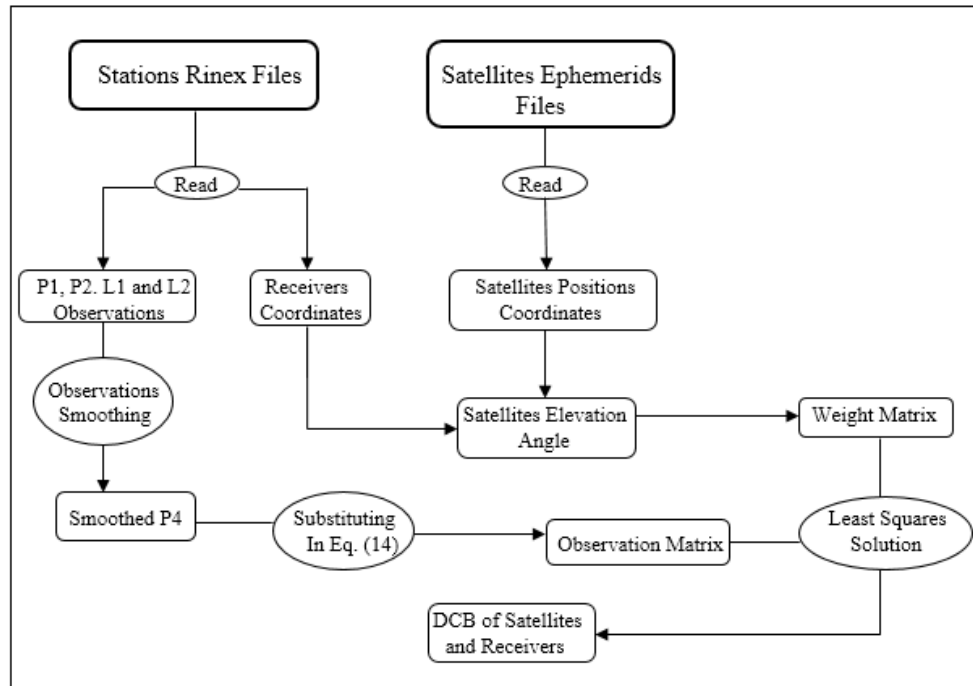
135 P is the weight matrix.

136 Each observation has a weight value depend on its satellite elevation angle. The weight value can be computed from the
 137 following equations (14, 15 and 18) (Luo X., 2013):

138 $w = \frac{\sigma_0^2}{\sigma^2}$ (14)

139 $\sigma^2 = \left[0.05 + \frac{0.02}{\sin(z)^2}\right]^2$ (15)

140 $\sigma_0^2 = (c + d)^2$ (16)



141
 142

Figure 1 Flow chart shows how the code works

143 **1. Mathematical Model Evaluation**

144 The MSDCBE software was written in MATLAB (version 2016a). The first input is GPS observations in Receiver Independent
 145 Exchange (RINEX) format according to the selected stations (figure 2) downloaded from (<ftp://garner.ucsd.edu/rinex>) and
 146 precise ephemerides (SP3) files of test days downloaded from (<http://www.GPScalendar.com/index.html?year=2010>). In
 147 addition, IONosphere Map EXchange Format (IONEX) files of IGS, CODE and JPL are downloaded - as a threshold values -
 148 from (<ftp://cddis.gsfc.nasa.gov/GPS/products/ionex/>).

149 In the present contribution, to evaluate the performance of the developed model, numerical case-studies were performed. The
 150 main goals of the numerical case-studies are to investigate three issues:

151 **First issue** is to investigate the effect of applying weighted least square instead of least square on satellites and GPS receiver
 152 DCBs, and this is done by comparing results from MSDCBE which applying weighted least square with the published results
 153 of M_DCB by Jin et al. (2012), and with those of IAAC.

154 BOGO, BRUS, GOPE, GRAS, ONSA, PTBB, SOFI and WTZA IGS Stations data from 1 to 31 January 2010 were applied as
 155 it was the same network used by Jin et al. (2012).

156 **Second issue** is to investigate the correlation between Size (number of receivers) of the GPS network and estimated DCBs for
 157 satellite and GPS receiver, and this is done by comparing a network consists of 3 GPS receiver and a network consists of 9
 158 GPS receiver.

159 This study was applied using IGS Stations data from 1 to 5 January 2010 of six stations namely, BOGO, BRUS, GOPE, GRAS,
 160 ONSA, PTBB, SOFI and WTZA.

161 **Third issue** is to investigate the congruence of DCBs estimated from absolute and relative methods with other IAAC, and this
 162 is done by comparing results from MSDCBE with the published results of ZDDCBE by Sedeek et al. (2017).

163 This study was applied using data from 1 to 5 January 2010 of six stations namely, GOPE, GRAS, ONSA, MADR, PTBB,
 164 and SOFI which was the same network used by Jin et al. (2012) and Sedeek et al. (2017).

165

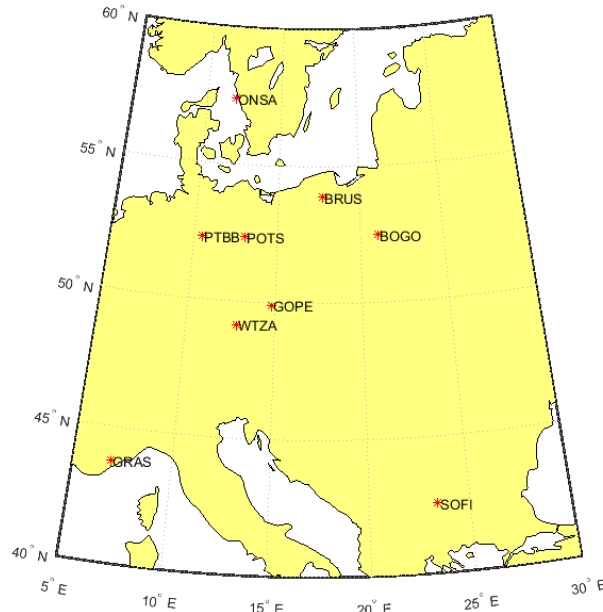


Figure 2 IGS Stations locations

166
 167

168 **Comparison of multi-station test results from MSDCBE and M_DCB**

169 The first evaluation made by this paper is the evaluation of weight function. MSDCBE used a weight function depending on
 170 the satellite elevation angle as mentioned before. Table 1 shows the differences and RMS between satellites and receivers
 171 estimated from 1 to 31 January 2010 using multiple GPS stations of both MSDCBE (weighted) and M_DCB (unweighted).

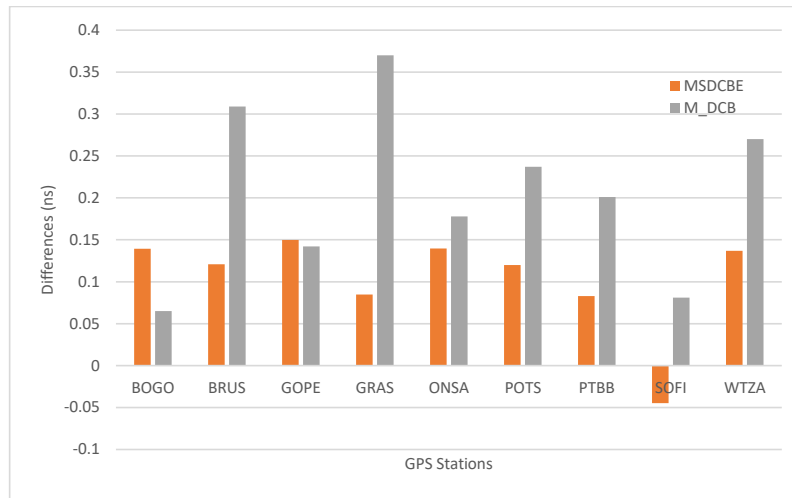
172 **Table 1** the differences and RMS between satellites and receivers estimated from 1 to 31 January 2010 using multiple GPS
 173 stations (MSDCBE and M_DCB minus CODE).

satellite	MSDCBE		M_DCB		satellite	MSDCBE		M_DCB	
	differences(ns)	RMS	differences(ns)	RMS		differences(ns)	RMS	differences(ns)	RMS
G1	0.228	0.250	0.746	0.251	G17	0.087	0.125	0.038	0.138
G2	0.121	0.091	-0.073	0.087	G18	-0.136	0.113	-0.044	0.100
G3	0.004	0.078	0.194	0.066	G19	0.236	0.095	0.381	0.066
G4	0.169	0.092	0.003	0.123	G20	0.096	0.096	0.004	0.073
G5	-0.082	0.106	-0.236	0.111	G21	-0.208	0.109	-0.121	0.088
G6	-0.059	0.066	0.169	0.061	G22	-0.188	0.091	0.050	0.109
G7	-0.015	0.084	-0.233	0.085	G23	0.210	0.082	0.052	0.053
G8	-0.094	0.085	-0.271	0.085	G24	-0.168	0.086	-0.221	0.076
G9	0.011	0.074	0.038	0.088	G25	-0.091	0.122	-0.220	0.085
G10	-0.068	0.088	-0.343	0.095	G26	-0.302	0.089	-0.020	0.092
G11	0.211	0.090	0.202	0.063	G27	0.078	0.062	0.060	0.088
G12	0.029	0.059	0.049	0.051	G28	-0.177	0.080	-0.340	0.107
G13	0.296	0.080	0.140	0.062	G29	-0.195	0.128	-0.277	0.091
G14	-0.058	0.124	0.150	0.126	G30	0.057	0.077	0.020	0.074
G15	-0.055	0.101	-0.164	0.117	G31	0.018	0.099	0.057	0.138
G16	-0.057	0.069	0.096	0.084	G32	0.102	0.070	0.115	0.077
BOGO	0.139	0.077	0.065	0.080	POTS	0.120	0.073	0.237	0.094
BRUS	0.121	0.120	0.309	0.111	PTBB	0.083	0.082	0.201	0.095
GOPE	0.150	0.069	0.142	0.068	SOFI	-0.045	0.119	0.081	0.113
GRAS	0.085	0.125	0.370	0.131	WTZA	0.137	0.078	0.270	0.083
ONSA	0.140	0.093	0.178	0.103					

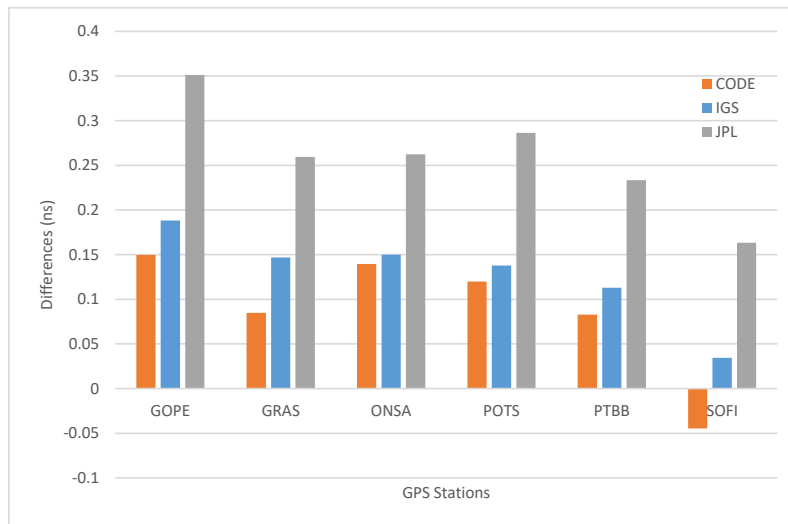
174 From the table one can see that the differences of BCD_C estimated satellites DCBs are less than 0.302 ns and the RMS of all
 175 satellites DCBs differences are less than 0.128 except G1 whose RMS = 0.250. The maximum difference of MSDCBE
 176 estimated receivers DCBs is 0.150 ns of receiver GOPE and the minimum is 0.045 ns of receiver SOFI (Figure 3). The
 177 maximum RMS of MSDCBE estimated receivers DCBs is 0.125. On the other side, M_DCB results show that Receiver DCB
 178 biases are slightly larger than those for satellites, but most of them are less than 0.4 ns except G1 whose DCB bias reaches
 179 0.746 ns. The RMS of all differences is lower than 0.3 ns (Jin et al. 2012). Figure 4 shows the mean differences between
 180 receiver DCB values estimated by MSDCBE and those released by CODE, IGS, and JPL combined from 1-31 Jan 2010. The



181 figure shows that the results of MSDCBE are mostly close to those of CODE than IGS and JPL. By comparing the figure 4
 182 with the corresponding chart published by Jin et al. (2012), it is clearly appeared that all differences between MSDCBE
 183 receivers' DCBs results and between CODE, IGS and JPL are less than those from M_DCB except station GOPE almost equal.



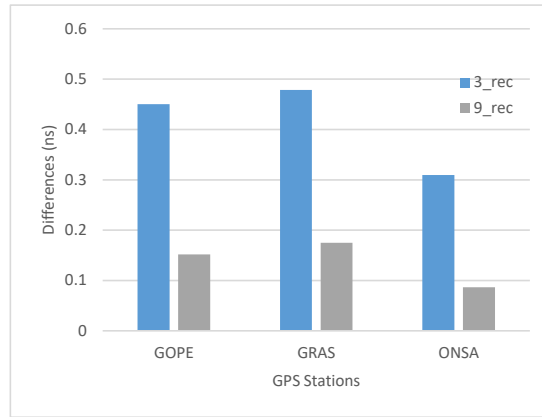
184
 185 **Figure 3** mean difference between the receiver DCB values of CODE and the computed values by each of M_DCB and
 186 N_DCB estimated from (1-31) Jan 2010.
 187



188
 189 **Figure 4** The mean differences between receiver DCB values estimated by MSDCBE and those released by CODE, JPL, and
 190 IGS combined from 1-31 Jan 2010.

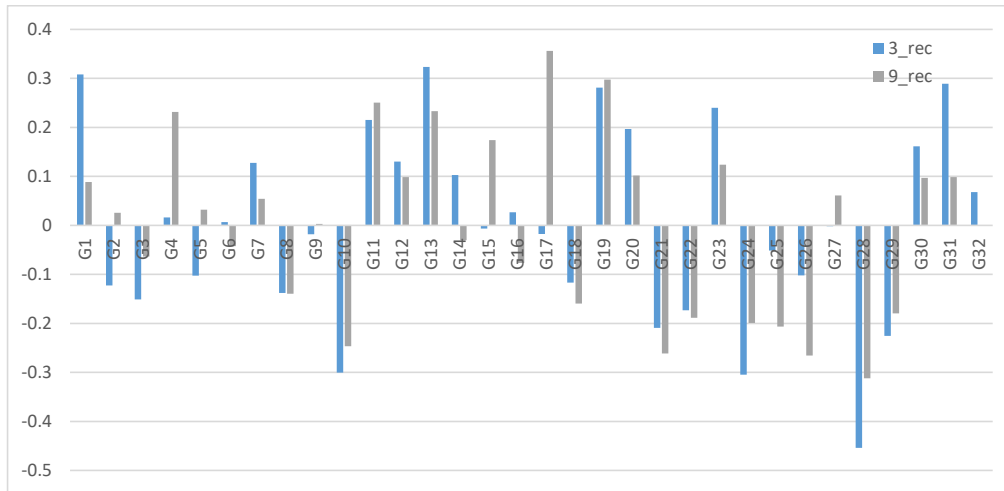
191 ***Effect of network size factor on DCB estimation***

192 By using multi station DCBs estimation, the number of stations used will appear as a factor influences DCBs estimation. This
 193 test was done by comparing DCBs computed by MSDCBE of a network of three receivers namely GOPE, GRAS, ONSA and
 194 DCBs of the same receivers but this time as a part of a network of nine receivers namely BOGO, BRUS, GOPE, GRAS,
 195 ONSA, PTBB, SOFI and WTZA. Figure 5 shows these results which demonstrate that using nine receivers gives more accurate
 196 DCBs. Also, the satellites DCBs differences (figure 6) almost improved but not like receivers DCBs, because satellites DCBs
 197 are small values compared with those of receivers.



198
 199
 200

Figure 5 mean difference between the receiver DCB values of IGS and the computed values by MSDCBE estimated from (1-5) Jan 2010.



201
 202
 203

Figure 6 mean difference between the satellites DCB values of IGS and the computed values by MSDCBE estimated from (1-5) Jan 2010

204

Comparison of multi-station from MSDCBE and single station from ZDDCBE and M_DCB test results

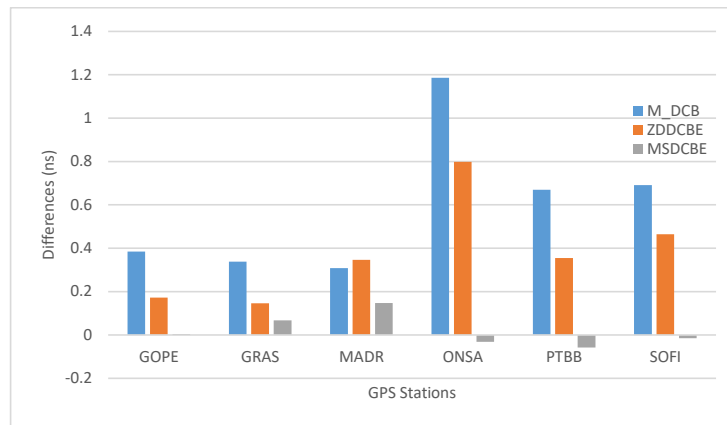
205
 206
 207
 208
 209
 210
 211

In this section the performance of multi station network against single station DCB estimation will be evaluated. Table 2 shows the mean difference between the receiver DCB values computed by IGS and the computed values by each of M_DCB, ZDDCBE and MSDCBE estimated from 1-5 Jan 2010. Figure 7 shows these results graphically and figure 8 shows the mean differences computed from M_DCB, ZDDCBE and MSDCBE for GPS satellites. The results show a significant difference between multi station network against single station DCB estimation. The maximum difference between receiver DCB estimation using IGS and MSDCBE is 0.1477 ns of MADR station, but it is 1.1866 ns and 0.7982 ns for M_DCB and ZDDCBE respectively.

212
 213

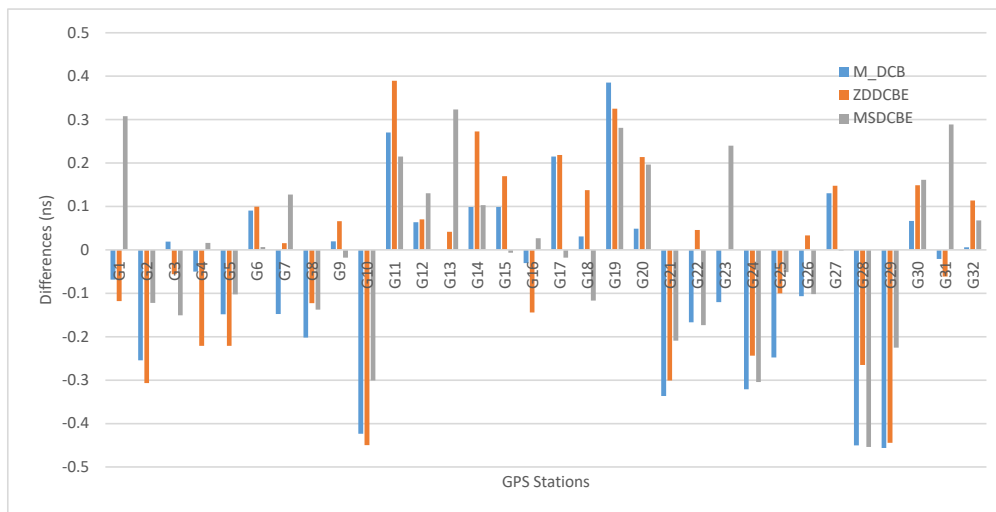
Table 2 Mean difference between the receiver DCB values computed by IGS and the computed values by using single station M_DCB, ZDDCBE and multi-station MSDCBE estimated from 1-5 Jan 2010.

IGS St.	Model	DCB diff. (ns)	IGS St.	Model	DCB diff. (ns)
GOPE	M_DCB	0.3847	ONSA	M_DCB	1.1866
	ZDDCBE	0.1724		ZDDCBE	0.7982
	MSDCBE	0.004		MSDCBE	-0.0310
GRAS	M_DCB	0.3379	PTBB	M_DCB	0.6692
	ZDDCBE	0.1466		ZDDCBE	0.3550
	MSDCBE	0.066		MSDCBE	-0.0578
MADR	M_DCB	0.3078	SOFI	M_DCB	0.6916
	ZDDCBE	0.3468		ZDDCBE	0.4650
	MSDCBE	0.1477		MSDCBE	-0.0149



214
 215
 216

Figure 7 mean difference between the receiver DCB values of IGS and the computed values by each of M_DCB, ZDDCBE and MSDCBE estimated from (1-5) Jan 2010



217
 218
 219

Figure 8 mean difference between the satellites DCB values of IGS and the computed values by M_DCB, ZDDCBE and MSDCBE estimated from (1-5) Jan 2010

220

Conclusions

221

The current study proposes a new MATLAB code called MSDCBE able to calculate DCBs of GPS satellites and receivers. This code was compared with two other codes and evaluated using IAAC data and from all the above, we can conclude that:

222

223

224

225

226

227

228

229

230

231

232

233

References

234

235

236

237

238

239

Abid, M., Mousa, A., Rabah, M., El mewafi, M., and Awad, A.: Temporal and spatial variation of differential code biases: A case study of regional network in Egypt, Faculty of Engineering, Alexandria University, Production and hosting by Elsevier B. V1110-0168, 2016.
 Al-Fanek, O.: Ionospheric Imaging for Canadian Polar Regions, PhD thesis, Calgary, Alberta, 2013.
 Ghilani, C., and Wolf, P.: Elementary surveying: an introduction to geomatics-13th ed, 2012.
 Haines, G.: Spherical cap harmonic analysis, J Geophys Res Solid Earth 1985;90(B3):2583e91, 1985.



- 240 Hansen, A.: Tomographic Estimation of the Ionosphere Using GPS Sensors, PhD Thesis, Department of Electrical
241 Engineering, Stanford University, CA, 2002.
- 242 Jin, R., Jin, S., and Feng, G.: M_DCB: MATLAB code for estimating GPS satellite and receiver differential code biases, GPS
243 Solution 16:541–548, 2012.
- 244 Jin, S., Luo, O., and Park, P.: GPS observations of the ionospheric F2-layer behavior during the 20th November 2003
245 geomagnetic storm over South Korea, *Journal of Geodesy*, 82(12):883–892, 2008.
- 246 Leandro, R.: Precise Point Positioning with GPS: A New Approach for Positioning, Atmospheric Studies, and Signal Analysis,
247 Ph.D. dissertation, Department of Geodesy and Geomatics Engineering, Technical Report No. 267, University of New
248 Brunswick, Fredericton, New Brunswick, Canada, 232 pp, 2009.
- 249 Leick, A., Rapoport, L., and Tatarnikov, D.: GPS satellite surveying, Wiley, New York, 2015.
- 250 Li, Z., Yuan, Y., Wang, N., Hernandez-Pajares, M., and Huo, X.: SHPTS: towards a new method for generating precise global
251 ionospheric TEC map based on spherical harmonic and generalized trigonometric series functions, *J Geodesy* 89(4):331–345,
252 2015.
- 253 Luo, X.: GPS Stochastic Modelling: Signal Quality Measures and ARMA Processes, PhD thesis, the Karlsruhe Institute of
254 Technology, Karlsruhe, Germany, 2013.
- 255 McCaffrey, A., Jayachandran, P., Themens, D., and Langley, R.: GPS receiver code bias estimation: A comparison of two
256 methods. Elsevier, *Advances in Space Research* 59 1984–1991, 2017.
- 257 Schaer, S.: Mapping and predicting the earth's ionosphere using global positioning system, Ph.D. dissertation, Astronomy
258 Institute, University Bern, Switzerland, 205 pp, 1999.
- 259 Sedeek, A., Doma, M., Rabah, M., and Hamama, M.: Determination of zero difference GPS differential code biases for
260 satellites and prominent receiver types, *Arab J Geosci*, DOI 10.1007/s12517-017-2835-1, 2017.
- 261 Zhang, B., Peter, J. G., Teunessen, Y., Hongxing, Z., and Min, L.: "Joint estimation of vertical total electron content (VTEC)
262 and satellite differential code biases (SDCBs) using low-cost receivers" *J. Geod.* 92: 401-413, 2018.
- 263